Integrating Transactive Energy Into Reliability Evaluation for a Self-Healing Distribution System With Microgrid

Jiaojiao Dong, *Senior Member, IEEE*, Lin Zhu, *Senior Member, IEEE*, Qihuan Dong, *Member, IEEE*, Paychuda Kritprajun, *Student Member, IEEE*, Yunting Liu, *Member, IEEE*, Yilu Liu, *Fellow, IEEE*, Leon M. Tolbert, *Fellow, IEEE*, Joshua C. Hambrick, *Member, IEEE*, Yaosuo Sonny Xue, *Senior Member, IEEE*, T. Ben Ollis, *Senior Member, IEEE*, Bishnu P. Bhattarai, *Senior Member, IEEE*, Kevin P. Schneider, *Fellow, IEEE*, and Stuart Laval, *Senior Member, IEEE*

***Abstract*—Non-utility owned distributed energy resources (DERs) are mostly untapped currently, but they can provide many grid services such as voltage regulation and service restoration, if properly controlled, and can improve the distribution system's reliability when coordinated with utility-owned assets such as self-healing control and microgrids. This paper integrates transactive energy control into the distribution system reliability evaluation to quantitatively assess the impact of non-utility owned DERs on reliability improvement. A transactive reactive power control strategy is designed to incentivize the DERs to provide reactive power support for improving voltage profiles thus enabling additional customer load restoration during an outage. Also, an operational sequence to coordinate the non-utility owned DERs with the utility owned self-healing control and utility owned microgrids is designed and integrated into the service restoration process with the operational constraints guaranteed by checking the three-phase unbalanced power flow for post-fault network reconfiguration. The reliability indices are then calculated through a Monte Carlo simulation. The transactive reactive power control strategy is tested on a four-feeder distribution system operated by Duke Energy in the U.S. Results demonstrate that the non-utility owned DERs with the transactive control improve the reliability of both the system and critical loads by more than 30%.**

***Index Terms*—Microgrids, power distribution, power system economics, power system reliability, power system restoration, transactive energy.**

Manuscript received March 12, 2021; revised June 22, 2021; accepted August 5, 2021. Date of publication August 18, 2021; date of current version December 16, 2021. This work was supported in part by the U.S. Department of Energy Grid Modernization Lab Consortium, by Engineering Research Center shared facilities supported by the Engineering Research Center Program of the National Science Foundation and the Department of Energy under NSF Award EEC-1041877, and by the CURENT Industry Partnership Program. Paper no. TSTE-00263-2021. *(Corresponding author: Lin Zhu.)*

Jiaojiao Dong, Lin Zhu, Qihuan Dong, Paychuda Kritprajun, and Yunting Liu are with the Department of Electrical Engineering and Computer Science, The University of Tennessee, Knoxville, TN 37996 USA (e-mail: jdong7@utk.edu; lzhu12@utk.edu; qdong7@utk.edu; pkritpra@vols.utk.edu).

Yilu Liu and Leon M. Tolbert are with the Department of Electrical Engineering and Computer Science, The University of Tennessee, Knoxville, TN 37996 USA, and also with the Oak Ridge National Laboratory, Oak Ridge, TN 37830 USA (e-mail: liu@utk.edu; tolbert@utk.edu).

Joshua C. Hambrick, Yaosuo Sonny Xue, and T. Ben Ollis are with the Oak Ridge National Laboratory, Oak Ridge, TN 37830 USA (e-mail: hambrickjc@ornl.gov; xuey@ornl.gov; ollistb@ornl.gov).

Bishnu P. Bhattarai and Kevin P. Schneider are with the Pacific Northwest National Laboratory, Seattle, WA 99354 USA (e-mail: bishnu.bhattarai@pnnl.gov; kevin.schneider@pnnl.gov).

Stuart Laval is with the Duke Energy, Charlotte, NC 28771 USA (e-mail: stuart.laval@duke-energy.com).

Color versions of one or more figures in this article are available at https://doi.org/10.1109/TSTE.2021.3105125.

Digital Object Identifier 10.1109/TSTE.2021.3105125

NOMENCLATURE

Parameters

B_d	Set of phases connected with phase *d*
C_{total}	Total electricity price ($/kWh)
C_{WL}	Wholesale electricity price ($/kWh)
C_{RT}	Retail price of electricity ($/kWh)
C_{ENS}	Energy not served cost to DSO ($/kWh)
C_{DNS}	Demand not served cost to DSO ($/kW)
G, B	Real and imaginary part of admittance matrix (S)
L_{ai}	Average customer load power at load point *I* (kW)
$MTTR_i$	Mean time to repair of component *i* (h)
N_T	Total number of customers
$\mathbf{N}, \mathbf{L}$	Set of nodes and set of branches
P_i^d	Active power of phase *d* at node *i* (kW)
Q_i^d	Reactive power of phase *d* at node *i* (kVar)
S_{inv}	Rated apparent power of the inverter (kVA)
$S_{ij,max}^d$	Capacity of the phase *d* of branch (*i*,*j*) (kVA)
t_0	Initial time instant of battery scheduling (h)
$V_{i,min}^d$	Lower bound of voltage of phase *d* at node *i* (V)
$V_{i,\max}^d$	Upper bound of voltage of phase *d* at node *i* (V)
ζ	Random value between 0 and 1
λ_i	Failure rate of component *i*
φ_i	Set of nodes that are connected with node *i*
Δt	Unit scheduling period of battery (h)
ΔT	Outage duration (h)

Variables

B_{DSO}	Benefits of the DSO ($)
C_{DER}	Cost of DERs ($)
$E_{battery}$	Required energy of battery (kWh)
MB_{DSO}	Marginal benefits of the DSO ($/kVar)

MC_{DER}	Marginal cost of DERs ($/kVar)
MC_{agg}	Aggregated marginal cost of DERs ($/kVar)
N_i	Number of interrupted customers in event *i*
P_{mg}	Total power output of a microgrid (kW)
P_{pv}	Power output of solar PV panels (kW)
$P_{battery}$	Power output of batteries (kW)
P_{backup}	Power output of backup generators (kW)
P_{ij}^{d}	Active power flow of phase *d* of branch (*i*,*j*) (kW)
P_{inv}	Active power operating point of the inverter (kW)
Q_{ij}^{d}	Reactive power flow of phase *d,* branch (*i*,*j*) (kVar)
Q_{inv}	Reactive power operating point of inverter (kVar)
Q_{DER}	Supplied reactive power by a DER (kVar)
Q_{DER}^{*}	Reactive power at market clearing point (kVar)
r_i	Interruption time for each event *i* (h)
TTF_i	Time to failure of component *i* (h)
TTR_i	Time to repair of component *i* (h)
U_i	Interruption duration at load point *i* (h)
V_i^{d}	Complex voltage phasor of phase *d* at node *i* (V)
ΔP_L	Additional load that can be restored (kW)

I. Introduction

DISTRIBUTION systems are becoming more complex and experiencing some fundamental changes, including the installation of an increasing number of intelligent devices and control systems to increase distribution system reliability and resilience against a high occurrence of faults and extreme weather [1]. Among the various assets, some are utility owned including distribution automation, self-healing controls, and microgrids while some are non-utility owned such as various types of distributed energy resources (DERs) including photovoltaic (PV) panels, electric vehicles, and behind-the-meter energy storage systems [2].

Using self-healing control and microgrids to improve the reliability and resilience for electric grids has been widely studied in recent years. An industry success of self-healing control is recently reported in [3], and a literature review of a self-healing distribution system is conducted in [4]. The use of microgrids as a reliability and resilience source is studied in [5]–[10] focusing on service restoration algorithms with microgrids as virtual feeders [5], [6], formulation of radiality constraints for microgrid formation after a disturbance [7], optimal operation of distribution systems with networked microgrids [8], [9], and optimal design of microgrids with battery and backup generators to improve resilience [10].

To further improve reliability and resilience, networked microgrids and their associated operation strategies are addressed in [11]–[13]. Ref [11] proposes a two-layer optimal consensus-based distributed control strategy to realize coordinated operation of networked microgrids under various operation objectives, e.g., frequency control, voltage control, and islanding and resynchronization of microgrids, etc. In [12], a division and unification control strategy is proposed to fully utilize microgrids' operational flexibility for improving resilience, where the networked microgrids are switched between a division mode and an unification mode depending on the operation stages. Also, a comprehensive review of distributed control and communication strategies in networked microgrids are conducted in [13]. These papers focus on the roles of utility owned assets, while the reliability benefits of non-utility owned DERs are rarely studied because of various challenges for existing control systems to directly control non-utility owned DERs [2], including accessibility for direct control, communication latency and bandwidth, widespread locations, and the large number of DERs, etc.

As a potential solution to engage non-utility owned DERs for various utility applications, transactive energy has attracted attention recently which provides incentive signals instead of direct control to incorporate the willingness of customers who own DERs to provide grid services [14]–[19]. Reference [14] proposed a theoretical framework to formulate a large class of transactive energy mechanisms. In the technical report [15], [16], the research team led by Pacific Northwest National Laboratory (PNNL) has conducted various use cases and validated the performance of transactive energy in voltage management under normal operating conditions. Reference [17] further conducted a proof-of-concept study to illustrate the capability of transactive energy to support service restoration in fault conditions. A distributed control agent for non-utility owned DERs is developed in [18] under the transactive energy control framework, and the associated aging effects of PV inverters when providing grid services are discussed in [19].

Non-utility owned DERs managed by transactive energy control can serve as a promising supplement to self-healing control and microgrids to further improve the reliability and resilience in future advanced distribution systems, especially after a bulk power grid outage or a severe fault with multiple load segments interrupted, where the utility-owned assets may not be enough to fully restore the customer loads without violating operational constraints. Therefore, there is an urgent need for distribution system planners and operators to evaluate the reliability benefits of non-utility owned DERs and build the confidence of transactive energy control deployment for utilities.

In recent years, research on distribution system reliability evaluation falls into three categories. The first category of research evaluates the impacts of many advanced techniques on distribution system reliability, including distributed generators [20], PV integration [21], microgrids [22] [23], recloser placement [24], self-healing control [25] [26], and outage management strategies [27].

The second category of research evaluates the impacts of several emerging issues on distribution system reliability, including the impact of malfunction of remotely controlled switches [28], availability of basic protection components [29], momentary events [30], cold load pickup events [31], multiple overhead feeders on the same tower [32], natural gas system interaction [33], and cyber faults [34].

The third category of research has focused on improving the reliability evaluation methods for various applications, for example, the fault incidence matrix based analytical method in [35] for reliability sensitivity analysis and reliability improvement planning, the non-simulation-based methods in [36]–[38] for

reliability constrained distribution system planning optimization problem, and the enhanced sampling methods in [39] to reduce the computation time in the sequential Monte Carlo simulation. Despite the above research, the reliability benefits of non-utility owned DERs has not been quantitively evaluated in the literature.

This paper proposes a comprehensive reliability evaluation framework for a self-healing multi-feeder distribution system with utility owned reclosers and microgrid and non-utility owned DERs, based on a sequential Monte Carlo simulation. The contributions of this paper are as follows. 1) The proposed method incorporates transactive energy control into reliability evaluation for the first time. 2) The transactive reactive power control strategy in a double-auction market to incentivize non-utility owned DERs for service restoration is evaluated on practical large distribution systems, and the impact of different penetration levels of DERs is demonstrated. 3) A detailed operational sequence is designed to coordinate the non-utility owned DERs and utility owned assets such as self-healing system and microgrids in service restoration, where the operational constraints are ensured by checking the three-phase unbalanced power flow solutions. 4) A case study on a practical four-feeder distribution system operated by Duke Energy in the U.S. is conducted, and results show that the reliability indices for both the whole system and the critical loads are improved using self-healing control, microgrid, and transactive energy. Especially, the engagement of non-utility owned DERs through transactive energy plays a significant role in improving the reliability of both the whole system and the critical loads.

The rest of the paper is organized as follows. In Section II, the mathematical model and work mechanism of the transactive energy are described. A detailed description of the proposed reliability evaluation framework is provided in Section III. Section IV gives the case study, and the conclusion is drawn in Section V.

II. Utilizing Transactive Energy of Non-Utility DERs for Reliability Improvement

This section describes the mathematical models and the working mechanism of the transactive reactive power control strategy to engage non-utility owned DERs to provide reactive power support, enable additional customer load service restoration during an outage, and therefore to improve the distribution system reliability.

A. Mathematical Model

The transactive reactive power control is implemented as a double auction market described below, including a distribution system operator (DSO) model, a DER model, and a market simulation model [17]. Here, DERs usually provide active power in the normal operation and will be engaged to provide reactive power for supporting service restoration after a fault.

1) DSO Model in Transactive Energy: The DSO model is used to generate a demand curve $MB_{DSO} = h_{DSO}(Q_{DER})$representing the marginal benefits that the DSO would receive from the reactive power support of DERs, as shown in (1).

$$MB_{DSO} = \frac{dB_{DSO}}{dQ_{DER}} \tag{1}$$

Since an explicit mathematical relationship $B_{DSO} = f(Q_{DER})$ is not available, the following two steps are taken to derive the relationship $\Delta P_L = f_1(Q_{DER})$ and $B_{DSO} = f_2(\Delta P_L)$, where f_1 is the load restoration curve representing the additional load that the DSO can restore as a function of the reactive power support, f_2 is a function that converts the load restoration amount into a dollar value. Therefore, $B_{DSO} = f_2(f_1(Q_{DER})) = f(Q_{DER})$.

First, the load restoration curve f_1 is calculated in an iterative manner by gradually increasing the reactive power Q_{DER} in small steps and computing the additional active power load that can be restored. For each small step, the three-phase unbalanced distribution network power flow equation is solved to check if the operational constraints are satisfied, including the voltage constraints for each node and the power flow constraints for each branch. Second, the relationship between the received benefits B_{DSO} and the additional customer load restoration ΔP_L is established in (2)-(3). The first term in (3) is the loss of revenue because of failing to serve the loads, the second term is the energy not served cost, and the third term is the demand not served cost.

$$B_{DSO} = C_{total}\Delta P_L \tag{2}$$

$$C_{total} = (C_{WL} - C_{RT})\,\Delta T + C_{ENS}\Delta T + C_{DNS} \tag{3}$$

2) DER Model in Transactive Energy*:* The DER model is used to generate a supply curve $MC_{DER} = h_{DER}(Q_{DER})$representing the marginal costs that the DERs incur for providing the reactive power support as shown in (4). An explicit mathematical relationship $C_{DER} = g(Q_{DER})$ is given in (5).

$$MC_{DER} = \frac{dC_{DER}}{dQ_{DER}} \tag{4}$$

$$C_{DER} = C_{RT}\left(\sqrt{S_{inv}^2 - Q_{inv}^2} - P_{inv}\right) - C_{RT}\left(\sqrt{S_{inv}^2 - (Q_{inv} + Q_{DER})^2} - P_{inv}\right) \tag{5}$$

3) Market Model in Transactive Energy: The transactive energy market is designed as a double auction market, and it receives both the demand curve submitted by the DSO and the supply curves by the DERs. This trading paradigm has been widely adopted in the conventional energy market. Also, it is adopted in [16] to engage distribution system assets for voltage management in Southern California Edison distribution feeders, and in [17] to engage DERs for improving distribution system service restoration. Since this paper focuses on engaging DERs to reduce the number and duration of customer interruption during outage events, the reaction time of auctions is assumed to be negligible compared with the interruption duration, which are usually several hours.

The multiple supply curves from all DERs are aggregated by the market to obtain a single supply curve and are then combined with the demand curve for market clearing. The feasibility of aggregating the supply curves is validated in [16] by case studies in Southern California Edison distribution feeders and by the implementation and demonstration in [18]. The detailed process of aggregation is described in [16] and briefly explained as follows. First, the pairs of reactive power amount and the marginal price for all supply curves are sorted in ascending order of the marginal price. Then, the available reactive power associated with the lowest marginal price will be taken. After the least expensive reactive power is completely allocated, the next portion of reactive power amount associated with the next lowest marginal price will be taken. Finally, this process is repeated until the maximum amount of reactive power is reached. Here, the maximum amount of reactive power could be either the total reactive power amount of submitted supply curves or the total demand, depending on which one is smaller. If the submitted reactive power exceeds the demand, then the extra reactive power amount will not be necessary to construct the aggregated supply curve. If the submitted reactive power amount does not meet the demand, then the restoration plan will need to be adjusted by removing some load segments such that the voltage can be maintained within the limits, i.e., only part of the interrupted load segments will be restored. Finally, the cleared reactive power Q^*_{DER} is determined by the intersection point of the demand curve and the supply curve in (6).

$$MB_{DSO}\left(Q^*_{DER}\right) = MC_{agg}\left(Q^*_{DER}\right) \tag{6}$$

B. Working Mechanism

During an outage, the transactive energy controller (TEC), which manages the non-utility owned assets for reactive power support, needs to coordinate with the distribution management system (DMS) which controls the utility assets (e.g., reclosers and microgrids). The coordination process is designed as follows. Here, Steps 1 and 3 are mainly conducted by the DMS, Step 2 is conducted by the TEC, and Step 4 is conducted by both DMS and TEC.

Step 1: When an outage happens, the DMS calculates an optimal reconfiguration strategy only considering utility assets and sends this reconfiguration strategy to the TEC.

Step 2: The TEC will run a double-auction market to calculate the incentive signals to engage the non-utility owned DERs and finds additional switching options.

Step 3: The DMS calculates new reconfiguration strategies that can restore additional loads.

Step 4: The reconfiguration strategy is executed by both the DMS and TEC, where the DMS controls the utility assets such as reclosers and microgrids, and the TEC sends incentive signals to engage the non-utility assets such as the DERs.

1) Operation of the Double-Auction Market: The operation of the double-auction market [14] in Step 2 is described to calculate the market clearing quantity of reactive power from the TEC. After the TEC receives the reconfiguration strategy from the DMS, the DSO and the DERs will generate the demand curve and supply curves respectively, as shown in Fig. 1. Then, the market clearing quantity is calculated as the intersection point of the demand curve and supply curve, where the supply curve is aggregated from that of all DERs. After that, the additional load restoration that is possible is calculated by substituting the clearing quantity of reactive power into the load restoration curve. Finally, the additional switching option is determined based on the additional load restoration amount, the total load of each segment, the topology and the priority level of each segment.

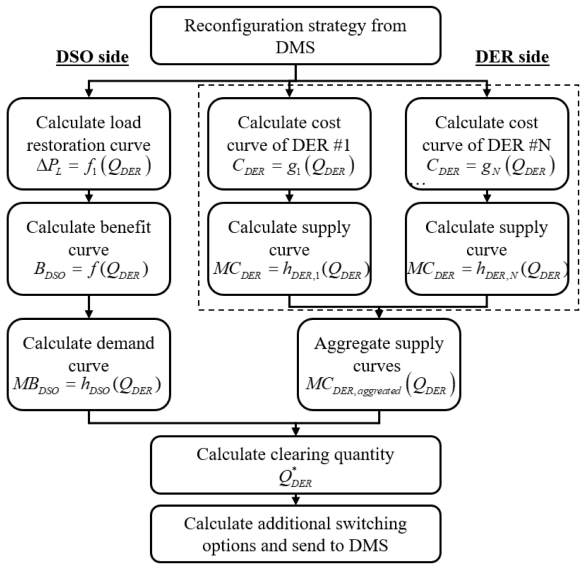

Fig. 1. The operation of the double-auction market.

The downstream load segment can be supplied only when the upstream load segment is connected, and the load segment with higher priority will be served first. Also, all loads in a given segment must be either fully restored, or not restored [17]. For example, considering there are two segments with the same priority level that need to be restored, and the load in one segment is 2 MW and the other segment is 1.5 MW. Assume there exists a restoration path for each load segment. If the additional load restoration amount is 4 MW, then both segments can be restored. But if the additional load restoration amount is 3 MW, then the larger load segment with 2 MW is restored while the 1.5 MW segment cannot be partially restored. This is because loads in the same segment can only be either fully restored or not restored. Here, the two steps of clearing the market and determining additional switching options are executed by the transactive energy controller, which is independent from the DSO and DERs, and could be owned by either the distribution system utility itself or a third party.

2) Operation of the DERs to Provide Reactive Power Support: The detailed operation of DERs for providing reactive power support is illustrated in Fig. 2 and explained as follows. The VOLTTRON^{TM} message bus and the Open Field Message Bus (OpenFMB) modules play important roles in this process. The OpenFMB module is the message bus to which many types of devices in the system can connect, including 1) the

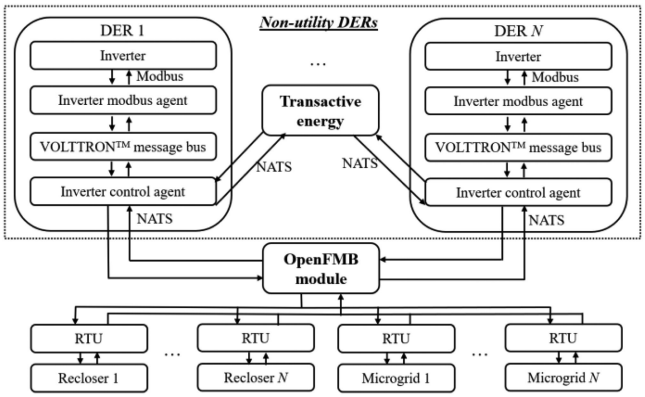

Fig. 2. Distributed control of DERs to enable reactive power support.

utility owned assets such as reclosers and microgrid, which are connected to the OpenFMB via remote terminal units (RTUs) and 2) non-utility owned assets such as DERs, which are connected to the OpenFMB via a VOLTTRON™ message bus, an open-source distributed control platform developed by PNNL [40]–[41].

To enable the DERs for providing reactive power support, three key elements are needed: 1) a transactive energy controller, 2) an inverter Modbus agent, which connects the VOLTTRON™ message bus and the inverters in each DER using Modbus TCP/IP protocol in order to monitor and control the DERs, and 3) an inverter control agent, which coordinates the VOLTTRON™ message bus, the transactive energy controller, and the OpenFMB module using the NATS publish-subscribe protocol.

At first, if the inverter control agent does not receive a signal from the transactive energy controller, it remains in the waiting state and will wait for the next market. If a signal from the transactive energy controller is received, the agent will construct the DER supply curve and send the curve to the transactive energy controller to participate in the market. Then, the agent will receive the cleared price from the transactive energy controller, and further calculate the reactive power amount to be supplied. Finally, the agent will send the reactive power amount to the VOLTTRON™ message bus, and further to the inverter Modbus agents to change the setpoints of DER inverters for providing reactive power support. More details of the inverter Modbus agent and inverter control agent and demonstrations of controlling DERs for providing reactive power support is presented in [18].

III. Reliability Evaluation Method With Self-Healing Control, Microgrid and Transactive Energy

With the market model and operation paradigm of transactive energy described in Section II, this section focuses on incorporating the transactive energy into the reliability evaluation method. To do so, the detailed operational sequence is needed to coordinate the non-utility owned DERs and utility owned assets such as self-healing system and microgrids in service restoration. Therefore, this section first describes the self-healing control and microgrid model in practical distribution systems. Then, the reliability evaluation method based on a time-sequential Monte Carlo simulation is proposed to incorporate the three emerging techniques, i.e., self-healing control, microgrid, and transactive energy.

A. Practical Distribution System With Self-Healing Control

Self-healing control typically features the capability of autonomous fault isolation and service restoration after a fault occurs. It can speed up the service restoration process and reduce the number and duration of customer interruptions, thus becoming an attractive technique for distribution system utilities to improve reliability and resilience in recent years. Self-healing control is enabled by advanced distribution automation protection devices such as smart switches, reclosers, and other remotely controlled switches as well as the associated communication and control technologies. These protection devices can either reconfigure the system automatically or can be controlled by operators remotely, and they act much faster than conventional manual switches, which can take a field crew several hours. In this paper, reclosers are considered as the key component to realize self-healing control, and they are also connected to the OpenFMB to publish their status update and subscribe to the status of other devices as shown in Fig. 2. Here, the three-phase unbalanced power flow equations in (7)-(9) are calculated to guarantee the operation constraints of voltage and line flow when maximizing the total restored loads in the service restoration. Equation (7) is the three-phase unbalanced power flow equation in rectangular coordinates, (8) is the voltage magnitude constraint, and (9) is the line flow constraint.

$$\begin{bmatrix} P_i^d \\ Q_i^d \end{bmatrix} = \begin{bmatrix} \mathrm{Im}(V_i^d) & \mathrm{Re}(V_i^d) \\ -\mathrm{Re}(V_i^d) & \mathrm{Im}(V_i^d) \end{bmatrix} \begin{bmatrix} \sum_{k\in\varphi_i}\sum_{t\in B_d}\left(G_{ik}^{dt}\mathrm{Im}(V_k^t)+B_{ik}^{dt}\mathrm{Re}(V_k^t)\right) \\ \sum_{k\in\varphi_i}\sum_{t\in B_d}\left(G_{ik}^{dt}\mathrm{Re}(V_k^t)-B_{ik}^{dt}\mathrm{Im}(V_k^t)\right) \end{bmatrix}, \quad \forall i\in\mathbf{N}, \forall d\in\{a,b,c\} \tag{7}$$

$$V_{i,\min}^d \le \left|V_i^d\right| \le V_{i,\max}^d, \forall i\in\mathbf{N},\ \forall d\in\{a,b,c\} \tag{8}$$

$$\left(P_{ij}^d\right)^2+\left(Q_{ij}^d\right)^2 \le \left(S_{ij,\max}^d\right)^2, \forall (i,j)\in\mathbf{L},\ \forall d\in\{a,b,c\} \tag{9}$$

B. Microgrid Model and Operation Mode

In addition to self-healing control, microgrids are also regarded as a potential way to improve system reliability and resilience, especially for ensuring reliable operation of critical loads (e.g., hospitals, emergency management centers, etc.). Typically, the power sources in a microgrid include PVs, batteries, and backup generators. The available power and energy that the microgrid can serve are given in (10) and (11) respectively, where the required energy of the battery is calculated from the battery power output and the time duration of a fault ΔT for batteries to supply power. Here, the required energy of the battery should be no more than the available battery capacity. More details about the models and operations of microgrids during a

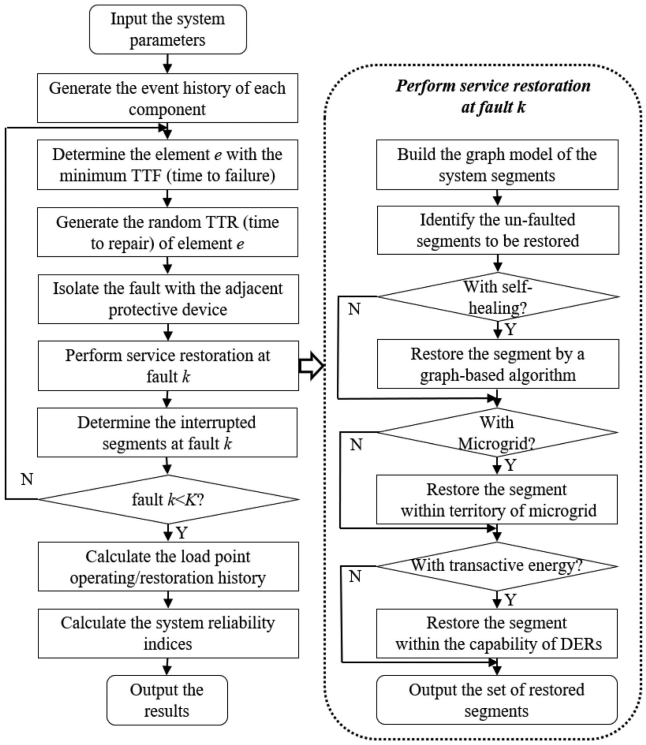

Fig. 3. Procedure of the distribution system reliability evaluation.

fault can be found in [10].

$$P_{mg}(t) = P_{pv}(t) + P_{battery}(t) + P_{backup}(t) \tag{10}$$

$$E_{battery} = \sum_{t=t_0}^{t_0+\Delta T} P_{battery}(t)\,\Delta t \tag{11}$$

When service restoration from a microgrid is desired, the microgrid controller needs to determine if it can supply power to a given segment for a required time period, and reports this to the centralized self-healing control. Then, the self-healing control re-evaluates the switching plan and instructs the microgrid to switch to islanded mode. Finally, the microgrid controller executes the islanding operation. The communication between the microgrid controller, the reclosers, and the centralized self-healing control can be realized by OpenFMB.

C. Reliability Evaluation Method With Three Advanced Techniques

The reliability evaluation procedure is shown in Fig. 3 and explained as follows. The input system parameters include system topology, load information, impedance of overhead lines and underground cables, and voltage operational constraints. Here, the impedance of the overhead lines and underground cables is used to compute the three-phase unbalanced power flow and ensure the voltage operation constraints are satisfied during the self-healing control. In this paper, the three-phase unbalanced power flow was solved using the MATLAB code in [24], [42]. Also, the locations of reclosers are needed for the service restoration using the self-healing system; the microgrid locations and territories are needed for the service restoration using the microgrids; and the locations and capacities of the non-utility DERs are also needed to capture the additional load restoration when engaging the transactive energy. Also, the input data for a sequential Monte Carlo simulation include the failure rate and repair time of both overhead lines and underground cables, which can be calibrated using the historical reliability indices in the utility. With these input data, the reliability evaluation method can calculate the reliability indices of the whole system and the critical loads.

The event history of each component is first generated using a time sequential Monte Carlo simulation after importing the system parameters, where the momentary faults are not considered in this paper. The operational history of each component is created in the time sequential Monte Carlo simulation as a two-state model, including the up state and the down state. The time during which the element remains in the up state, i.e., the time to failure (TTF) is generated by (12), and the time during which the element is in the down state, i.e., the time to repair (TTR) is generated by (13) [20].

$$TTF_i = \frac{\ln(\zeta)}{\lambda_i} \times 8760 \tag{12}$$

$$TTR_i = -\ln(\zeta) \times MTTR_i \tag{13}$$

For each fault event k in $\{1, 2, \ldots, K\}$, where K is the total number of events, the fault isolation and service restoration are performed to identify the interrupted load sections during the event. The faults happening at a lateral branch are isolated by a fuse, and the customers are restored after the fuse is replaced. The faults happening at the main trunk are isolated by reclosers, followed by the restoration process.

To incorporate the three emerging techniques, i.e., self-healing control, microgrid, and transactive energy, the service restoration process needs to be modified compared with the conventional reliability analysis procedure, as shown in the right part of Fig. 3. Also, the operational sequence of the service restoration using the three advanced techniques is designed and described in detail below.

First, a three-phase to ground fault happens at fault k. An example of this fault type would be a tree falling across the line and contacting the ground. Based on the fault location, the adjacent protective devices (e.g., reclosers, circuit breakers, etc.) sense the fault current and operate based on the local protection settings. The faulted segment will remain in a non-energized (isolated) state until the faulted line is repaired. The centralized self-healing control evaluates the current system condition and designs several restoration paths that satisfy the voltage operational constraints. In this paper, a heuristic method based on a graph representation of the segment model is adopted to find feasible restoration strategies with details described in [25]. In addition, the existing service restoration algorithms based on the mathematical optimization in the literature are also compatible with the proposed reliability evaluation method. A comprehensive review of service restoration algorithms is presented in [43].

The microgrid controller also checks its available power and energy and evaluates if it can support the territory for a required time period. The microgrid will report it to the DSO and wait

for islanding signals to switch to islanded mode if it can support its territory during the fault.

Furthermore, if the non-utility DERs are available, the transactive energy control is engaged. A double auction market is established with the demand curve submitted by the DSO and the supply curves by the DERs. With market clearing, the additional switching option is determined and sent back to the DSO to restore additional load segments. With these three advanced techniques, both the restored and interrupted load segments are determined for the reliability calculation. The reliability indices are then calculated from the customer interruptions of all generated events.

Utilities typically utilize a set of indices [44] to evaluate the system reliability, e.g., System Average Interruption Duration Index (SAIDI), System Average Interruption Frequency Index (SAIFI), etc. The SAIFI in (14) shows the frequency that the average customer experiences a sustained interruption over a predefined time period. The SAIDI in (15) shows the total duration of interruption for the customers during a predefined period. It is usually calculated in minutes or hours of customer interruption. There are also other reliability indices, e.g., average service availability index (ASAI), average service unavailability index (ASUI), energy not served (ENS), and average energy not served (AENS) [45], given in (16)-(19) respectively.

$$SAIFI = \sum\nolimits_i N_i / N_T \tag{14}$$

$$SAIDI = \sum\nolimits_i r_i N_i / N_T \tag{15}$$

$$ASAI = (8760 - SAIDI)/8760 \tag{16}$$

$$ASUI = 1 - ASAI \tag{17}$$

$$ENS = \sum\nolimits_i L_{ai} U_i \tag{18}$$

$$AENS = ENS / N_T \tag{19}$$

IV. Case Study on a Duke Energy Distribution System

The studied Duke Energy distribution system has four feeders operating at 12.47 kV, named as Feeder 1, 2, 3, 4, respectively. These four feeders are supplied by two substations as shown in [2]. There are two rooftop solar PV sites and a microgrid site with 2 MW of solar and batteries to serve critical loads in the system. Also, the system has four circuit breakers and 12 reclosers that have been installed or are being installed, where RCL2, RCL7, RCL9 and RCL11 are normally open tie switches while the others are normally closed sectionalizing switches. The voltage operational constraint is selected based on the range A of the allowable ANSI C84.1 [46], where the voltage across the network is between 0.95 p.u. to 1.05 p.u.

A. Circuit Model and Segmentation

Table I shows the basic information of each feeder, including the number of nodes, the number of lines, the contained segments, the number of loads, the total line length in miles, the total load power in MW, and the total number of customers.

TABLE I
Basic Information of Each Feeder

Feeder	F1	F2	F3	F4
Nodes	393	386	604	634
Lines	392	385	603	633
Segments	S0-S1	S2-S6	S7-S9	S10-S11
Loads	175	164	292	273
Length (miles)	8.12	12.93	19.35	18.01
Power (MW)	2.79	6.59	6.41	7.78
Total customers	434	470	974	1294

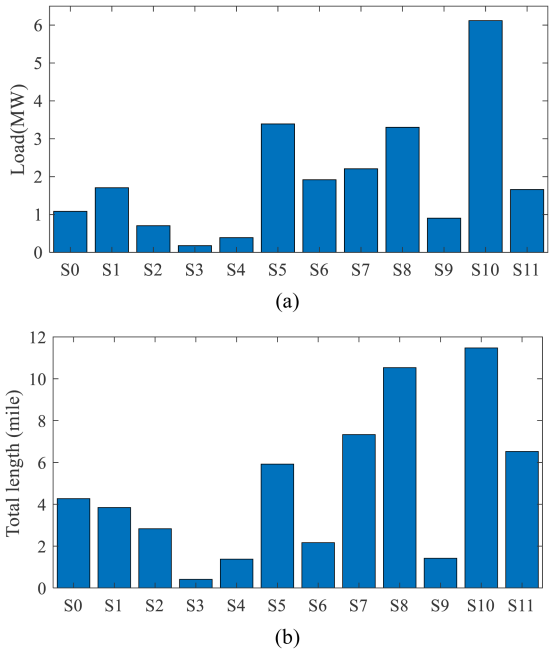

Fig. 4. Statistic data of each segment, (a) load distribution among each segment and (b) line length distribution among each segment.

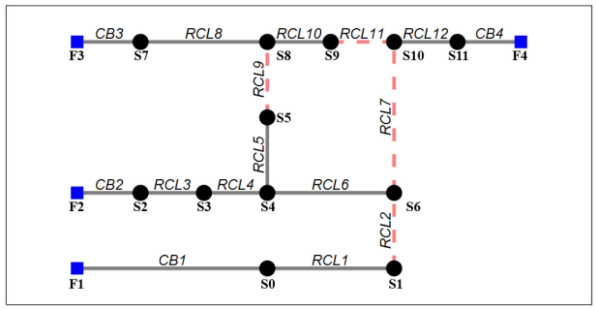

Fig. 5. Segment model under normal condition.

Fig. 4 shows the load distribution and line length distribution for each segment.

The system segment model is represented as a single-line diagram in Fig. 5, where the blue squares mean the substation node of each feeder, the black dots mean segments, the solid line means closed reclosers while the dashed lines mean open reclosers. Here, S3 and S4 are the critical load segments.

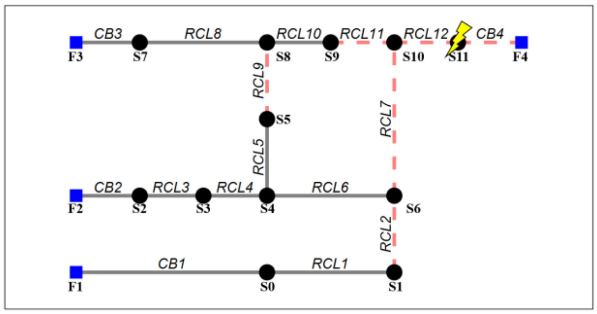

Fig. 6. Segment model after fault isolation.

B. Reactive Power Support From Transactive Energy

Assuming a permanent fault happens in S11, it is isolated by opening CB4 and RCL12. The system segment model after fault isolation is shown in Fig. 6. The faulted segment S11 will be in an outage state until the faulted line is repaired. Also, S10 will lose power and need to be restored by adjacent feeders. Since the loading of S10 is relatively high, it cannot be restored by any of the other three feeders if only using utility-owned assets since the voltage constraints will be violated after picking up S10. Therefore, non-utility DERs need to be engaged to enable the restoration of S10. For illustration, Feeder 3 is selected to pick up S10.

Fig. 7 shows the detailed operation of the transactive energy. From the load restoration curve in Fig. 7(a), the demand curve in Fig. 7(b) is calculated by the marginal benefit that the DSO can receive from reactive power support. Then, from the supply curve of each DER in Fig. 7(c), the aggregated supply curve in Fig. 7(d) is calculated. Both the demand curve and the supply curve are inputs to the double-auction market. Fig. 7(e) shows the market clearing point for this case is (2791 kVar, 0.048 \$/kVar), computed by the intersection of the demand curve and aggregated supply curve. It means the DSO and DERs are willing to trade reactive power for 2791 kVar at the price of 0.048 \$/kVar. The cleared reactive power is mapped on the load restoration curve to calculate the actual amount of the load that can be restored for the given cleared reactive power value. From Fig. 7(a), these reactive supports can help restore an additional 6670 kW of load, which is larger than the load amount of S10. Therefore, S10 could be fully restored after engaging the non-utility DERs through transactive energy. The additional restored load segment S10 is 25.96% of the total load in the whole system, and the total load in Feeder 3 under this new configuration is increased by 95.41%.

Fig. 8 shows the voltage profile for the new configuration of Feeder 3 before and after engaging the non-utility owned DERs through transactive energy. Before using transactive energy, Feeder 3 has a low-voltage issue when picking up the large load in segment S10, and the minimum voltage magnitude is around 0.92 p.u. But after using the transactive energy, the voltage is within the limit (0.95 p.u.) because the non-utility DERs are used to provide reactive power support and improve the voltage profile.

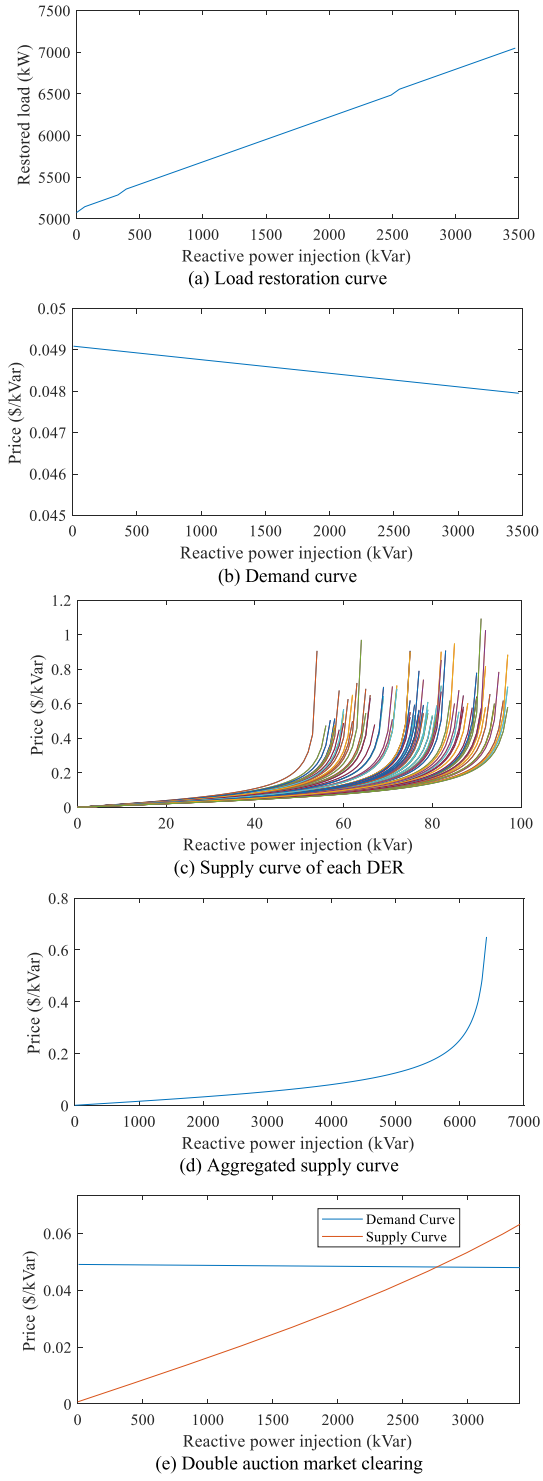

Fig. 7. Detailed operation of the transactive energy.

C. Service Restoration Strategies Under all Fault Locations

A sequence of events in a 10-year time period is generated by a time sequential Monte Carlo simulation to mimic the behavior of the practical distribution system. Fig. 9 shows the histogram of the simulated faults among the segments.

Table II gives the different scenarios' settings, where the base case means the traditional distribution systems with manual

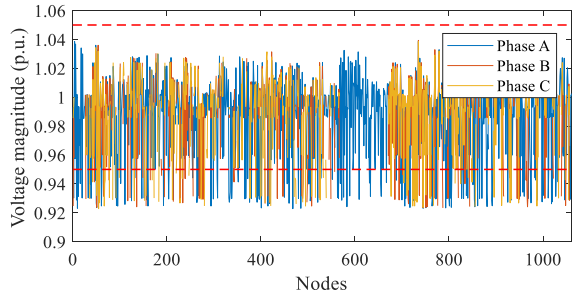

(a) Without transactive energy

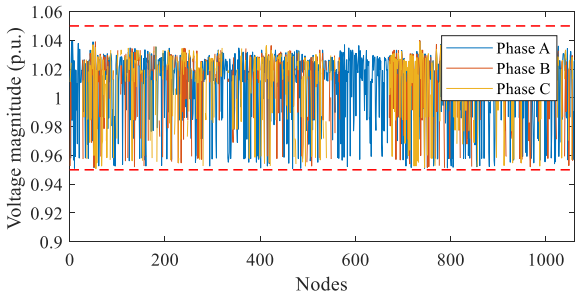

(b) With transactive energy

Fig. 8. Voltage profile of Feeder 3 when restoring S10.

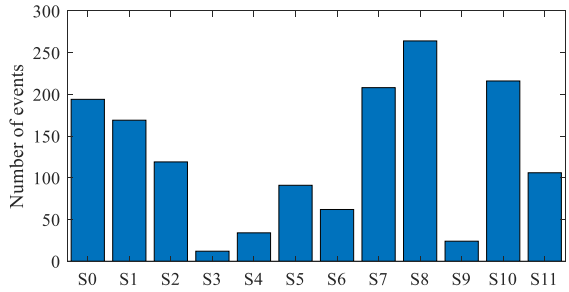

Fig. 9. Histogram of the simulated faults.

TABLE II
SCENARIO SETTINGS

Scenario	Manual switches	Reclosers & self-healing	Microgrid	Transactive energy
Base case	√	--	--	–
# 1	–	√	--	–
# 2	–	√	√	–
# 3	–	√	√	√

switches only and the time for manual switching operation is set as 1.5 hours [47] in the case study. Table III summarizes the restoration results of all the possible fault locations under the scenarios in Table II. For Scenario 3 with transactive energy, we further investigated different penetration levels of DERs that can participate in the transactive energy control to be more practical. It shows that with higher penetration of DERs, the more reactive power can be provided, thus improving the voltage profile and enabling the restoration of additional load segments. By gradually increasing the DER penetration level, which is the percentage of total DER capacity in the total load of the four feeders, we obtained the following results: 1) when the DER penetration level reaches 10%, S4 can be restored by

TABLE III
SUMMARY OF SERVICE RESTORATION FOR ALL THE SCENARIOS

Scenario	Non-restored segments	Details
Base case	S3, S4, S8, S10	--
# 1	S3, S4, S8, S10	--
# 2	S8, S10	S3 & S4 by microgrid
# 3: 10% DER	S8, S10	S3 & S4 by transactive energy
# 3: 20% DER	S10	S8 by transactive energy
# 3: 60% DER	–	S10 by transactive energy

TABLE IV
RELIABILITY OF THE WHOLE SYSTEM

Scenario	SAIFI	SAIDI	SAIFI↓	SAIDI ↓
Base case	12.99	63.06	–	--
# 1	11.45	61.24	11.85%	2.89%
# 2	11.42	61.10	12.09%	3.11%
# 3: 10% DER	11.42	61.10	12.09%	3.11%
# 3: 20% DER	10.05	54.97	22.64%	12.83%
# 3: 60% DER	7.96	43.14	38.72%	31.59%

"↓" means the percentage of reduction.

transactive energy, even without the microgrid; 2) when the DER penetration level reaches 20%, S8 can be further restored; and 3) when the DER penetration level reaches 60%, S10 can also be restored.

D. Reliability Improvement in a Self-Healing Distribution System With Microgrid and Transactive Energy

Table IV shows the reliability indices of the whole system as well as the reliability improvement compared with the base scenario. It shows that Scenario 1 with self-healing control can reduce the SAIFI by 11.85%, since the deployment of reclosers and self-healing control can enable the capability of autonomous service restoration after an outage. Furthermore, Scenario 3 with transactive energy can greatly improve the system reliability, for example, the SAIFI and SAIDI can be reduced by 38.72% and 31.59% from the base case respectively if the DER penetration levels reaches 60%. These results demonstrate the great potential of transactive energy combined with self-healing control in improving the whole system level reliability. For Scenario 2 with microgrid, the reliability indices of the whole system do not have significant improvement compared with Scenario 1 with self-healing control only. This is because the size of the microgrid is relatively small and is mainly used to serve the critical load. Therefore, the microgrid will greatly improve the reliability of the critical load as intended, but would only have a small impact on the whole system.

Table V shows the reliability indices of the critical load as well as the reliability improvement compared with the base scenario. It shows that Scenario 1 with self-healing control does not improve the critical load reliability due to the lack of available service restoration path. For all other scenarios, there exists a path to restore the critical load segment S4, either by the microgrid in Scenario 2 or by the transactive energy in Scenario 3, so the reliability indices of the critical load segment are greatly improved by the microgrid or the transactive energy.

TABLE V
RELIABILITY OF THE CRITICAL LOAD

Scenario	SAIFI	SAIDI	SAIFI↓	SAIDI ↓
Base case	6.59	30.50	–	--
# 1	6.59	30.50	–	--
# 2	4.02	16.38	39.00%	46.30%
# 3: 10% DER	4.02	16.38	39.00%	46.30%
# 3: 20% DER	4.02	16.38	39.00%	46.30%
# 3: 60% DER	4.02	16.38	39.00%	46.30%

TABLE VI
ADDITIONAL RELIABILITY INDICES OF THE WHOLE SYSTEM

Scenario	ASAI	ASUI	ENS	AENS
Base case	0.9928	0.0072	22737	7.17
# 1	0.9930	0.0070	21495	6.78
# 2	0.9930	0.0070	21378	6.74
# 3: 10% DER	0.9930	0.0070	21378	6.74
# 3: 20% DER	0.9938	0.0062	19291	6.08
# 3: 60% DER	0.9951	0.0049	14781	4.66

TABLE VII
ADDITIONAL RELIABILITY INDICES OF THE CRITICAL LOAD

Scenario	ASAI	ASUI	ENS	AENS
Base case	0.9965	0.0035	198.11	7.08
# 1	0.9965	0.0035	198.11	7.08
# 2	0.9981	0.0019	106.33	3.80
# 3: 10% DER	0.9981	0.0019	106.33	3.80
# 3: 20% DER	0.9981	0.0019	106.33	3.80
# 3: 60% DER	0.9981	0.0019	106.33	3.80

E. Discussions

Regarding the scalability, the proposed reliability evaluation method is tested on a practical distribution system with more than 2000 nodes, and it is also capable to deal with larger size distribution systems. Since the distribution system is usually operated in a segment manner, the segment model based on switch locations is widely used in finding the service restoration strategies. The number of segments is usually much smaller than the number of nodes in distribution systems, which makes the service restoration process scalable. After feasible service restoration strategies are calculated, the full model is used to solve the three-phase power flow and check the voltage violations for all nodes. Also, the distributed control implementation of transactive energy is scalable to engage a large number of and widespread locations of DERs in practical distribution systems. In addition, the needed DER penetration level in Table III could be slightly different under different selections of DER locations in order to restore the same number of load segments, while the reliability indices will only be changed when the restored load segments are different.

The voltage operational constraint in the previous case study is selected based on the range A of the allowable ANSI C84.1 [47], where the voltage across the network is between 0.95 p.u. to 1.05 p.u. If a tighter or looser voltage range is selected, then the service restoration strategies in Table III for different penetration levels of DERs may be slightly changed. For example, if the voltage range is tighter, then it becomes harder for the service restoration strategies to meet the voltage constraints. As a result, there may be additional non-restored segments in Table III other than S3, S4, S8 and S10, for both the base case and Scenario 1. Then, the non-restored segments will also be more than S8 and S10 for Scenario 2 and Scenario 3, which will need higher penetration levels of DERs to restore these possible additional segments. Similarly, if the voltage range is looser, then a lower penetration level of DERs is sufficient to restore the same number of load segments.

The size of the microgrid in the previous case study is no less than the amount of the critical load, and it can support the critical load when needed. If the microgrid is larger, it will not impact the reliability results as long as it only serves the critical load within its territory. But if the microgrid is smaller, there may exist some events during which the available power of the microgrid does not meet the demand of the critical loads. This will not impact the reliability of the whole system much in Table IV, since the critical load is a small portion compared with the total load in the whole system. However, the reliability of the critical load will be lower in Table V for Scenario 2 and Scenario 3. Specifically, the SAIFI of the critical load in Scenario 2 and Scenario 3 will be between 4.02 and 6.59, and the SAIDI will be between 16.38 and 30.50. Also, a higher penetration level of DERs will be needed to restore the critical load in this case.

Two reliability indices, i.e., SAIFI and SAIDI are calculated for demonstration in the previous case study, and the proposed method can also be used to calculate other widely used reliability indices. Tables VI and VII further give the ASAI, ASUI, ENS, and AENS of all the scenarios, for both the whole system and critical loads. The result shows these reliability indices are also greatly improved after engaging the non-utility owned DERs.

V. CONCLUSION

This paper proposes a comprehensive reliability evaluation framework that integrates three advanced techniques: self-healing control, microgrid, and transactive energy with non-utility owned DERs. Different from existing research, this paper integrates a transactive reactive power control strategy in the reliability evaluation for the first time to quantitatively analyze the impact of non-utility owned DERs on distribution system reliability. An operational sequence is designed to coordinate the non-utility owned DERs with the utility owned self-healing system and microgrids in service restoration, and the detailed three-phase unbalanced power flow is considered to ensure the feasibility of restoration strategies. The case study is conducted on a practical distribution system with four feeders operated by Duke Energy. Results show that the reliability indices of both the whole system and the critical loads are improved using the combined self-healing control, microgrid, and transactive energy. Especially, the engagement of non-utility owned DERs through transactive energy demonstrates great potential in improving the reliability of distribution systems. In the future work, the impact of the communication failure on the practical distribution system reliability is worth further analyzing.

REFERENCES

[1] C. Chen, J. Wang, and D. Ton, "Modernizing distribution system restoration to achieve grid resiliency against extreme weather events: An integrated solution," *Proc. IEEE,* vol. 105, no. 7, pp. 1267–1288, Jul. 2017.

[2] K. P. Schneider *et al.*, "A distributed power system control architecture for improved distribution system resiliency," *IEEE Access*, vol. 7, pp. 9957–9970, Jan. 2019.

[3] Municipal utility's grid improves by 50% with self-healing technology, Accessed: May 8, 2017. [Online]. Available: https://www.sandc.com.br/globalassets/sac-electric/documents/sharepoint/documents-all-documents/case-study-766-1001.pdf?dt=637476604571022061

[4] R. M. Campos, C. C. Figueroa, H. V. Oyarzun, and J. M. Baeza, "Self-healing of electric distribution networks: A review," in *Proc. 7th Int. Conf. Comput. Commun. Control*, 2018, pp. 63–70.

[5] J. Li, X. Y. Ma, C. C. Liu, and K. P. Schneider, "Distribution system restoration with microgrids using spanning tree search," *IEEE Trans. Power Syst.,* vol. 29, no. 6, pp. 3021–3029, Nov. 2014.

[6] M. Khederzadeh and S. Zandi, "Enhancement of distribution system restoration capability in single/multiple faults by using microgrids as a resiliency resource," *IEEE Syst. J.,* vol. 13, no. 2, pp. 1796–1803, Jun. 2019.

[7] S. Lei, C. Chen, Y. Song, and Y. Hou, "Radiality constraints for resilient reconfiguration of distribution systems: Formulation and application to microgrid formation," *IEEE Trans. Smart Grid,* vol. 11, no. 5, pp. 3944–3956, Sept. 2020.

[8] Z. Wang, B. Chen, J. Wang, and C. Chen, "Networked microgrids for self-healing power systems," *IEEE Trans. Power Syst.*, vol. 7, no. 1, pp. 310–319, Jan. 2015.

[9] Z. Wang and J. Wang, "Self-healing resilient distribution systems based on sectionalization into microgrids," *IEEE Trans. Power Syst.,* vol. 30, no. 6, pp. 3139–3149, Nov. 2015.

[10] J. Dong, L. Zhu, Y. Su, Y. Ma, Y. Liu, F. Wang, L. M. Tolbert, J. Glass, and L. Bruce, "Battery and backup generator sizing for a resilient microgrid under stochastic extreme events," *IET Gener. Transm. Distrib.,* vol. 12, no. 20, pp. 4443–4450, 2018.

[11] Q. Zhou, Z. Tian, M. Shahidehpour, X. Liu, A. Alabdulwahab, and A. Abusorrah, "Optimal consensus-based distributed control strategy for coordinated operation of networked microgrids," *IEEE Trans. Power Syst.*, vol. 35, no. 3, pp. 2452–2462, May 2020.

[12] Q. Zhou, M. Shahidehpour, A. Alabdulwahab, and A. Abusorrah, "Flexible division and unification control strategies for resilience enhancement in networked microgrids," *IEEE Trans. Power Syst.*, vol. 35, no. 1, pp. 474–486, Jan. 2020.

[13] Q. Zhou, M. Shahidehpour, A. Paaso, S. Bahramirad, A. Alabdulwahab, and A. Abusorrah, "Distributed control and communication strategies in networked microgrids," *IEEE Commun. Surv. Tut.*, vol. 22, no. 4, pp. 2586–2633, Sep. 2020.

[14] S. Li, J. Lian, A. J. Conejo, and W. Zhang, "Transactive energy systems: The market-based coordination of distributed energy resources," *IEEE Control Syst. Mag.,* vol. 40, no. 4, pp. 26–52, Aug. 2020.

[15] J. Lian, Y. Sun, K. Kalsi, S. E. Widergren, D. Wu, and H. Ren, "Transactive system: Part II: Analysis of two pilot transactive systems using foundational theory and metrics," Tech. Rep. PNNL-27235, Pacific Northwest National Lab.(PNNL), Richland, WA, 2018.

[16] M. J.E. Alam, A. Somani, R. B. Melton, and T. E. McDermott, "Transactive approach for engaging distribution network assets for voltage management in Southern California Edison distribution feeders," Tech. Rep. PNNL-27650, Pacific Northwest National Lab.(PNNL), Richland, WA, 2018.

[17] B.P. Bhattarai, J. Alam, J. Hansen, K. Schneider, N. Radhakrishnan, A. Somani, and W. Du, "Enhancing distribution system resiliency through a novel transactive energy systems framework," in *Proc. IEEE Power Energy Soc. Gen. Meeting*, 2019, pp. 1–5.

[18] P. Kritprajun, J. C. Hambrick, L. M. Tolbert, J. Dong, L. Zhu, Y. Liu, B. Bhattarai, K. Schneider, and S. Laval, "VOLTTRON$^{\mathrm{TM}}$ agent development for enabling reactive power support of non-utility DERs by integrating transactive energy approach," in *Proc. IEEE Power Energy Soc. Gen. Meeting*, 2020, pp. 1–5.

[19] Y. Liu, P. Kritprajun, L. M. Tolbert, J. Dong, L. Zhu, J. C. Hambrick, K. Schneider, and B. P. Bhattarai, "Modeling of marginal cost for PV inverter ancillary services considering inverter aging under transactive energy framework," in *Proc. IEEE Power Energy Soc. Gen. Meeting*, Aug. 2020, pp. 1–5.

[20] F. Li and N. Sabir, "Monte Carlo simulation to evaluate the reliability improvement with DG connected to distribution systems," in *Proc. 8th WSEAS Int. Conf. Electric Power Syst., High Voltages, Electric Machines*, 2008, pp. 21–23.

[21] S. Su, Y. Hu, L. He, K. Yamashita, and S. Wang, "An assessment procedure of distribution network reliability considering photovoltaic power integration," *IEEE Access,* vol. 7, pp. 60171–60185, May 2019.

[22] Z. Bie, P. Zhang, G. Li, B. Hua, M. Meehan, and X. Wang, "Reliability evaluation of active distribution systems including microgrids," *IEEE Trans. Power Syst.,* vol. 27, no. 4, pp. 2342–2350, Nov. 2012.

[23] J. L. López-Prado, J. I. Vélez, and G. A. Garcia-Llinás, "Reliability evaluation in distribution networks with microgrids: Review and classification of the literature," *Energies,* vol. 13, no. 23, 2020, Art. no. 6189.

[24] J. Dong, L. Zhu, Y. Liu, and D. T. Rizy, "Enhancing distribution system monitoring and resiliency: A sensor placement optimization tool (SPOT)," in *Proc. IEEE Power Energy Soc. Gen. Meeting*, Aug. 2019, pp. 1–5.

[25] J. Dong *et al.*, "Quantitative evaluation of reliability improvement: case study on a self-healing distribution system," in *Proc. IEEE Power Energy Soc. Innov. Smart Grid Technol. Conf.*, Feb. 2020, pp. 1–5.

[26] J. R. Aguero, "Applying self-healing schemes to modern power distribution systems," in *Proc. IEEE Power Energy Soc. Gen. Meeting*, Jul. 2012, pp. 1–4.

[27] H. Farzin, M. Fotuhi-Firuzabad, and M. Moeini-Aghtaie, "Role of outage management strategy in reliability performance of multi-microgrid distribution systems," *IEEE Trans. Power Syst.,* vol. 33, no. 3, pp. 2359–2369, May 2018.

[28] A. Safdarian, M. Farajollahi, and M. Fotuhi-Firuzabad, "Impacts of remote control switch malfunction on distribution system reliability," *IEEE Trans. Power Syst.,* vol. 32, no. 2, pp. 1572–1573, Mar. 2016.

[29] A. S. Nazmul Huda and R. Zivanovic, "Study effect of components availability on distribution system reliability through multilevel monte carlo method," *IEEE Trans. Ind. Inform.,* vol. 15, no. 6, pp. 3133–3142, Jun. 2019.

[30] P. Gautam, P. Piya, and R. Karki, "Development and integration of momentary event models in active distribution system reliability assessment," *IEEE Trans. Power Syst.,* vol. 35, no. 4, pp. 3236–3246, Jul. 2020.

[31] A. Al-Nujaimi, M. A. Abido, and M. Al-Muhaini, "Distribution power system reliability assessment considering cold load pickup events," *IEEE Trans. Power Syst.,* vol. 33, no. 4, pp. 4197–4206, Jul. 2018.

[32] K. Xie, K. Cao, and D. C. Yu, "Reliability evaluation of electrical distribution networks containing multiple overhead feeders on a same tower," *IEEE Trans. Power Syst.,* vol. 26, no. 4, pp. 2518–2525, Nov. 2011.

[33] Z. Zeng, T. Ding, Y. Xu, Y. Yang, and Z. Dong, "Reliability evaluation for integrated power-gas systems with power-to-gas and gas storages," *IEEE Trans. Power Syst.,* vol. 35, no. 1, pp. 571–583, Jan. 2020.

[34] W. Liu, Q. Gong, H. Han, Z. Wang, and L. Wang, "Reliability modeling and evaluation of active cyber physical distribution system," *IEEE Trans. Power Syst.,* vol. 33, no. 6, pp. 7096–7108, Nov. 2018.

[35] C. Wang, T. Zhang, F. Luo, P. Li, and L. Yao, "Fault incidence matrix based reliability evaluation method for complex distribution system," *IEEE Trans. Power Syst.,* vol. 33, no. 6, pp. 6736–6745, Nov. 2018.

[36] G. Muñoz-Delgado, J. Contreras, and J. M. Arroyo, "Reliability assessment for distribution optimization models: A non-simulation-based linear programming approach," *IEEE Trans. Smart Grid*, vol. 9, no. 4, pp. 3048–3059, Jul. 2016.

[37] Z. Li, W. Wu, B. Zhang, and X. Tai, "Analytical reliability assessment method for complex distribution networks considering post-fault network reconfiguration," *IEEE Trans. Power Syst.,* vol. 35, no. 2, pp. 1457–1467, Aug. 2020.

[38] A. Tabares, G. Munoz-Delgado, J. F. Franco, J. M. Arroyo, and J. Contreras, "An enhanced algebraic approach for the analytical reliability assessment of distribution systems," *IEEE Trans. Power Syst.,* vol. 34, no. 4, pp. 2870–2879, Jul. 2019.

[39] G. T. Heydt and T. J. Graf, "Distribution system reliability evaluation using enhanced samples in a Monte Carlo approach," *IEEE Trans. Power Syst.,* vol. 25, no. 4, pp. 2006–2008, Nov. 2010.

[40] J. Haack *et al.*, "VOLTTRON$^{\mathrm{TM}}$: Using distributed control and sensing to integrate buildings and the grid," in *Proc. IEEE 3rd World Forum Internet Things*, Dec. 2016, pp. 228–232.

[41] J. Haack, B. Akyol, N. Tenney, B. Carpenter, R. Pratt, and T. Carroll, "VOLTTRON$^{\mathrm{TM}}$: An agent platform for integrating electric vehicles and smart grid," in *Proc. Int. Conf. Connected Veh. Expo.*, 2013, pp. 81–86.

[42] A. Garces, "A linear three-phase load flow for power distribution systems," *IEEE Trans. Power Syst.*, vol. 31, no. 1, pp. 827–828, Jan. 2016.

[43] F. Shen, Q. Wu, and Y. Xue, "Review of service restoration for distribution networks," *J. Mod. Power Syst. Clean Energy,* vol. 8, no. 1, pp. 1–14, Jan. 2020.

[44] *IEEE Guide for Electric Power Distribution Reliability Indices*, IEEE Standard 1366, 2004.

[45] L. Chen and J. He, *Power system reliability: Principles and applications*, 2nd ed. Beijing, China: Tsinghua Univ. Press, 2015, pp. 321–324.
[46] ANSI C84.1 electric power systems and equipment - voltage ranges, Accessed: Apr. 02, 2011. [Online]. Available: http://www.powerqualityworld.com/2011/04/ansi-c84-1-voltage-ratings-60-hertz.html
[47] Y. Xu, C. Liu, K. P. Schneider, and D. T. Ton, "Placement of remote-controlled switches to enhance distribution system restoration capability," *IEEE Trans. Power Syst.*, vol. 31, no. 2, pp. 1139–1150, Mar. 2016.

Jiaojiao Dong (Senior Member, IEEE) received the B.S. degree in information engineering from Xi'an Jiaotong University, Xi'an, China, and the M.S. and Ph.D. degrees in automation control from the same university, in 2008, 2011, and 2016, respectively. She is currently a Postdoctoral Researcher with the University of Tennessee, Knoxville, TN, USA. Her research interests include power system planning and operation, renewable energy integration, and microgrids.

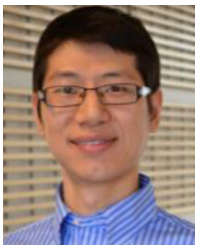

Lin Zhu (Senior Member, IEEE) received the B.S. and Ph.D. degrees in electrical engineering from the Huazhong University of Science and Technology, Wuhan, China, in 2005 and 2011, respectively. He is currently a Research Assistant Professor with the Min H. Kao Department of Electrical Engineering and Computer Science, University of Tennessee, Knoxville (UTK), TN, USA. Earlier, he was a Research Associate and Postdoc with UTK. His current research interests include power system dynamics, renewable energy integration, smart distribution grid, and microgrid.

Qihuan Dong (Member, IEEE) received the bachelor's degree from Electronic Engineering Department, Fudan University, Shanghai, China, in 2014 and the Ph.D. degree in electrical engineering from the University of Cambridge, Cambridge, U.K., in 2019. Previously, she was a Postdoctoral Research Associate with the University of Tennessee, Knoxville, TN, USA. Her research interests include electric applications of high temperature superconductors (HTS), especially superconducting fault current limiters, and power system reliability and resilience.

Paychuda Kritprajun (Student Member, IEEE) received the B.S. degree in electrical engineering from the King Mongkut's Institute of Technology Ladkrabang, Thailand, in 2014, and the M.S. degree in 2020 in electrical engineering from the University of Tennessee, Knoxville, TN, USA, where she is currently working toward the Ph.D. degree. She was a Design Engineer with Nissan Motor Asia Pacific Co., Ltd., Thailand, in 2014 and an Electrical Engineer with Provincial Electricity Authority (PEA), Thailand, during 2015–2018. Her research interests include PV systems, renewable energy integration, and microgrids.

Yunting Liu (Member, IEEE) received the B.S. degree in electrical engineering from the Huazhong University of Science and Technology, Wuhan, China and the Ph.D. degree in electrical engineering from Michigan State University, East Lansing, MI, USA, in 2013 and 2019, respectively. In 2019, she joined the University of Tennessee, Knoxville, TN, USA, as a Postdoctoral Research Associate. In 2021, she joined Michigan Technological University, Houghton, USA, as an Assistant Professor. Her research interests include modular multilevel converter, renewable energy integration, and power converter aging analysis.

Yilu Liu (Fellow, IEEE) received the B.S. degree in electrical engineering from Xi'an Jiaotong University, Xi'an, China, and the M.S. and Ph.D. degrees in electrical engineering from The Ohio State University, Columbus, OH, USA, in 1986 and 1989, respectively. She was a Professor with Virginia Tech, Blacksburg, VA, USA, where she led the effort to create the North American Power Grid Frequency Monitoring Network, which is currently operated with The University of Tennessee, Knoxville (UTK), TN, USA, and Oak Ridge National Laboratory (ORNL), Oak Ridge, TN, USA, as GridEye. She is currently a Governor's Chair with UTK and ORNL. She is also the Deputy Director of the DOE/NSF-Co-Funded Engineering Research Center, Center for Ultra-Wide-Area Resilient Electric Energy Transmission Networks (CURENT). Her current research interests include power system wide-area monitoring and control, large interconnection-level dynamic simulations, electromagnetic transient analysis, and power transformer modeling and diagnosis. She is a Member of the U.S. National Academy of Engineering and the National Academy of Inventors.

Leon M. Tolbert (Fellow, IEEE) received the bachelor's, M.S., and Ph.D. degrees in electrical engineering from the Georgia Institute of Technology, Atlanta, GA, USA, in 1989, 1991, and 1999, respectively.

He is currently a Chancellor's Professor and the Min H. Kao Professor with the Department of Electrical Engineering and Computer Science, The University of Tennessee, Knoxville, TN, USA. He is a Founding Member and Testbed Thrust Leader of the NSF/DOE Engineering Research Center, CURENT (Center for Ultra-wide-area Resilient Electric Energy Transmission Networks). He is also an Adjunct Participant with Oak Ridge National Laboratory, Oak Ridge, TN, USA. His research interests include the utility applications of power electronics, microgrids, electric vehicles, and wide bandgap semiconductors.

Dr. Tolbert is a Registered Professional Engineer in the state of Tennessee. He was the recipient of the 2001 IEEE Industry Applications Society Outstanding Young Member Award, and eight prize paper awards from the IEEE Industry Applications Society and IEEE Power Electronics Society. He was an Associate Editor for the IEEE TRANSACTIONS ON POWER ELECTRONICS from 2007 to 2013 and the Paper Review Chair for the Industry Power Converter Committee of the IEEE Industry Applications Society from 2014 to 2017. He is currently an Academic Deputy Editor-in-Chief of the IEEE POWER ELECTRONICS MAGAZINE during 2021–2023.

Joshua C. Hambrick (Member, IEEE) received the B.S., M.S., and Ph.D. degrees in electrical engineering from Virginia Tech, Blacksburg, VA, USA. He was a R&D Staff Member with Oak Ridge National Laboratory in the Power and Energy Systems Group until 2021. His research interests include power systems modeling and simulation, power systems protection, and microgrid design and control. Dr. Hambrick is active in number of standards activities, including the IEEE 1547 and IEEE 2030 series of standards.

Yaosuo Sonny Xue (Senior Member, IEEE) received the B.Sc. degree in electrical engineering from East China Jiaotong University, Nanchang, China and the M.Sc. degree in electrical engineering from the University of New Brunswick, Fredericton, NB, Canada, in 1991 and 2004, respectively. From 1991 to 2000, he was an Electrical Engineer-in-Charge with China Railway Design Corporation and led the traction power systems R&D for the first high-speed electric railway in China. During 2005–2006, he was with Capstone Turbine Corporation, as a Lead Power Electronics and Systems Engineer. He was with Siemens Corporate Research from 2009 to 2015 and led Corporate Technology North America power electronics and energy management program. He is currently with Oak Ridge National Laboratory, Oak Ridge, TN, USA, and his research interests include multilevel converters and smart inverter controls for renewable energy and utility applications. He is an Associate Editor for the IEEE TRANSACTION ON POWER ELECTRONICS, IEEE JOURNAL OF EMERGING AND SELECTED TOPICS IN POWER ELECTRONICS, and IEEE OPEN ACCESS JOURNAL OF POWER AND ENERGY.

T. Ben Ollis (Senior Member, IEEE) received the B.S. and M.S. degrees in electrical engineering from the University of Tennessee, Knoxville, TN, USA, in 2012 and 2014, respectively. He is currently an R&D Staff Member and a Power System Research Engineer with Oak Ridge National Laboratory, Oak Ridge, TN, USA. He has been a Member of ORNL since 2013 and is currently with Grid Components and Controls Group. He has utility experience as a Planning Engineer with Duke Energy and as a Power System Operator with Clinton Utilities Board. He currently leads research projects focused on small- and large-scale microgrids, networked microgrids, grid resiliency, device interoperability, and novel energy generation technologies.

Bishnu P. Bhattarai (Senior Member, IEEE) received the Ph.D. degree in electrical engineering from Aalborg University, Aalborg, Denmark, in 2015. He is currently a Senior Research Scientist/Engineer with Pacific Northwest National Laboratory, USA. His research interests include advanced modeling and simulation of power distribution systems, transactive energy system, and power and communication co-simulations. He was the recipient of the Gold Medal from the President of Nepal in 2011, Green Talent Awards from the German Federal Ministry of Education and Research in 2017, and Best Reviewer Awards from Elsevier IJEPES in 2017 and from IEEE TRANSACTIONS ON SMART GRID in 2018 and 2019. He is currently the Editor of the IEEE TRANSACTIONS ON SMART GRID.

Kevin P. Schneider (Fellow, IEEE) received the B.S. degree in physics and the M.S. and Ph.D. degrees in electrical engineering from the University of Washington, Seattle, WA, USA. He is currently a Chief Engineer with Pacific Northwest National Laboratory, the Manager of the Distribution and Demand Response Sub-Sector, and a Research Professor with Washington State University as part of the PNNL/WSU Advanced Grid Institute (AGI). He is an Affiliate Associate Professor with the University of Washington and a licensed Professional Engineer with Washington State. His research interests include distribution system analysis and power system operations. He is a Past Chair of the Power & Energy Society (PES) Distribution System Analysis (DSA) Sub-Committee, and the past Chair of the Analytic Methods for Power Systems (AMPS) Committee.

Stuart Laval (Senior Member, IEEE) received the bachelor's and master's degrees in electrical engineering and computer science from MIT, the M.B.A. degree from the Rollins College, and the Ph.D. degree in industrial engineering from the University of Central Florida, Orlando, FL, USA. He is currently a Member of Duke Energy's Emerging Technology Office, where he leads the development of grid-edge operational technologies and pioneering utility interoperability standards. He has more than 15 years of experience in the development of more than 30 technology solutions in electric utility power systems, telecommunications, and power electronics.